NDT&E International 83 (2016) 88–93

Contents lists available at ScienceDirect

NDT&E International

journal homepage: www.elsevier.com/locate/ndteint

Inspection of stress corrosion cracking in welded stainless steel pipe using point-focusing electromagnetic-acoustic transducer

Nobutomo Nakamura *, Kazuhiro Ashida, Takashi Takishita, Hirotsugu Ogi, Masahiko Hirao

Graduate School of Engineering Science, Osaka University, 1–3 Machikaneyama, Toyonaka, Osaka 560–8531, Japan

ARTICLE INFO

Article history:
Received 2 May 2016
Received in revised form
15 June 2016
Accepted 16 June 2016
Available online 18 June 2016

Keywords:
Electromagnetic acoustic transducer
Point focusing
SV wave
Weld
Stress corrosion cracking

ABSTRACT

Point-focusing electromagnetic-acoustic transducers (PF-EMATs) for shear-vertical (SV) waves were developed for crack inspection of stainless-steel pipes. The transducer has improved defect detectability by accumulating SV waves generated by concentric line sources at a focal point in phase. An optimum frequency for defect detection was found to be 2 MHz, with which a crack of 0.5 mm depth near a weld was clearly detected. The EMAT exhibited defect detectability comparable to that of a conventional phased-array piezoelectric transducer, indicating that this new EMAT is highly practical for the non-contacting evaluation of stress-corrosion cracking in stainless steels.

1. Introduction

Stress-corrosion cracking (SCC) around welds is the critical failure of stainless-steel pipes in chemical and power plants, and nucleation and growth of cracks are routinely inspected by the ultrasonic testing (UT). Crack size is normally estimated from amplitude of ultrasonic waves (echoes) reflected by the cracks. For monitoring crack growth with this method, however, reproducibility of the amplitude measurement must be guaranteed. High signal-to-noise (*S*/*N*) ratio is also required to detect small cracks in the early stage.

With piezoelectric transducers, echo amplitude is highly affected by the measurement conditions such as surface roughness of specimens and contacting pressure between a specimen and transducers. These features lower the reproducibility of the amplitude measurement, making inspection of degradation over time unreliable. In addition, a requirement of coupling materials restricts an inspection with moving transducers by robots. In contrast, an electromagnetic acoustic transducer (EMAT) [1–4] allows the noncontact operation, being free from coupling materials. Ultrasonic-wave sources are generated directly in inspected materials, and echo amplitude is not affected by the contacting pressure. It is also insensitive to the surface roughness. These are advantages over the piezoelectric transducers, and there are studies using EMATs for several industrial purposes, [5–10] in addition to the crack inspection. [11,12].

The *S*/*N* ratio of an EMAT is generally smaller than that of a piezoelectric transducer. However, it has been overcome by increasing strain energy density using the focusing [13–15] and the resonant [16] techniques, by which weak elastic waves are superimposed in phase to produce a high enough intensity. In this study, we design an advanced EMAT utilizing the former technique for crack inspection of stainless-steel pipes. By focusing shear vertical (SV) waves generated from several circular line sources of an EMAT at a focal point, the *S*/*N* ratio and spatial resolution are improved, making detection of small cracks possible. We developed a SV-wave point-focusing EMAT (PF-EMAT), and confirmed its ability for detecting slit defects deeper than 0.05 mm [17,18]. As the operating frequency increases, smaller cracks will be detected, although attenuation due to scattering by grains becomes significant. Thus, an optimum driving frequency should exist for the crack inspection with the PF-EMAT. In this study, we developed PF-EMATs operating at different frequencies between 1.1 and 3.0 MHz, and evaluated their defect detectability and spatial resolution for stainless steels. Then, cracks artificially fabricated near a weld in a stainless-steel pipe were inspected, and applicability of the developed PF-EMAT for crack inspection was discussed.

2. Experiments

2.1. PF-EMAT

The developed EMAT consists of two identical concentric meander-line coils and magnets as shown in Fig. 1(a). Hand-

* Corresponding author.
E-mail address: nobutomo@me.es.osaka-u.ac.jp (N. Nakamura).

http://dx.doi.org/10.1016/j.ndteint.2016.06.005
0963-8695/

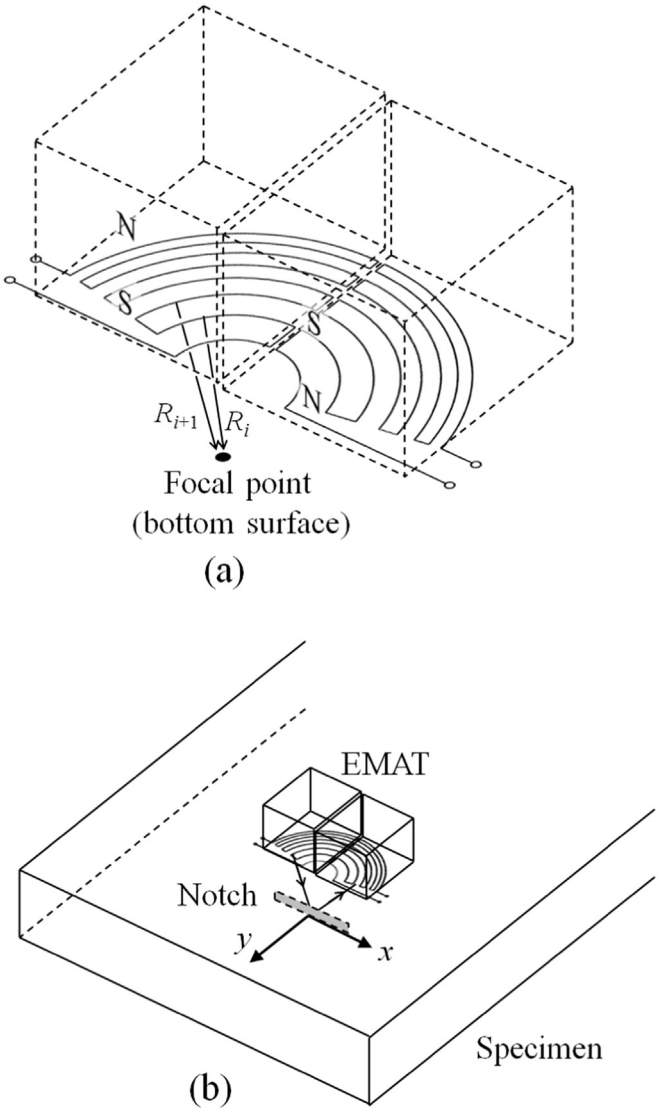

Fig. 1. (a) Configuration of the PF-EMAT, and (b) the coordinate system in the specimen.

wound coils are placed on a specimen surface, and rectangular parallelepiped magnets oppositely polarized are placed on them. The EMAT is operated by inputting burst currents into one of the coils. The currents generate eddy currents on the specimen surface, and the Lorentz forces are generated parallel to the specimen surface and normal to the coil, which are sound sources of SV waves. The SV waves generated on the specimen surface are reflected by cracks on the bottom surface, and the reflected waves are detected by the other coil.

An SV wave radiated from a narrow line source vibrating parallel to a specimen surface and perpendicular to the line source shows unique directivity. Amplitude and phase vary depending on the radiation angle, θ, from the normal direction to the specimen surface. [19] In a stainless-steel specimen, amplitude is nearly constant from 0° to 30°, shows a peak around 32°, drops to zero at 45°, and becomes less than 13% of the maximum above 45°. [18] The phase is unchanged between 0 and 32°, and it varies above 32°.

Point focusing is performed by using interference of SV waves generated by a meander-line coil. Current direction in the meander-line coil is alternative between the neighboring segments, and phases of SV waves radiated from the segments are different by π, half cycle. When the SV waves radiated from each segment arrive at a focal point in phase, the amplitude is enhanced and the point focusing is performed. Spacing between the segments is determined so that difference in the length of the propagation paths from the neighboring sources to the focal point equals the half of the wavelength λ, $R_{i+1} - R_i = \lambda/2$, where R_i is the distance between the focal point and ith segment (Fig. 1(a)). We designed EMATs with the radiation angles less than 37.5° so as to neglect the angle dependence of the phase. The shear-wave velocity of stainless steel was set to be 3100 m/s.

We used plate specimens with 20 mm thickness and a pipe specimen with 35 mm thickness as described later. We fabricated five PF-EMATs operated at 1.1, 1.5, 2.0, 2.5, and 3.0 MHz for the plate specimens. The cycles of the driving burst signal were 4 at 1.1 MHz, 8 at 1.5 MHz, and 12 at other frequencies, so that the driving signal did not overlap the signal of SV waves reflected by cracks. Amplitude of the received signal was determined by gating out the intended signal and using a superheterodyne technique. The number of segments were 4, 5, 7, 8, and 10 in 1.1, 1.5, 2.0, 2.5, and 3.0 MHz EMATs, respectively. Size of the coils was about 15 mm by 15 mm. Focal points of the EMATs were set to be on the bottom surface of the specimens with 20 mm thickness; the depth of the focal point corresponded to the thickness of the specimens. For the pipe inspection, we designed a 2 MHz PF-EMAT whose focal depth was 35 mm. The number of cycles of the driving burst signal was set to be 20, and the number of segments was 10.

2.2. Specimens

Notches with rectangular cross section were fabricated by an electric discharge machine on back surfaces of stainless steel (SUS304) plates with thickness of 20 mm. The notch width and length were 0.5 mm and 10 mm, respectively, and the depth, d, ranged from 0.05 to 2.95 mm. A welded stainless-steel specimen was also prepared. The specimen, a curved plate, including welded region was cut from a stainless steel (SUS316) welded pipe, and stress corrosion cracks were introduced beside the weld metal on the inner surface by applying bending stress in a corrosion solution. Outer diameter and thickness around the welded region were 600 and 35 mm, respectively. Excess weld metal on the outer surface was removed. In the following discussion, x and y axes were defined parallel to and normal to, respectively, the notch for the plate specimen and the weld line for the pipe specimen (Fig. 1(b)).

3. Results and discussion

3.1. Frequency dependences of notch detectability and spatial resolution

Fig. 2 shows representative waveforms averaged over 16 shots obtained by using the 2 and 3 MHz PF-EMATs from a flawless region and from the notch of 0.8 mm depth. In the waveform at 3 MHz from a flawless region, a signal is observed at the gate position; a similar signal is observed also for 2.5 MHz PF-EMAT. Its amplitude is almost unchanged when the EMATs are moved in flawless regions, and the signal is expected to originate from acoustic waves that are reflected at the bottom surface (the origin is not completely understood yet). The signal overlaps with echoes from notches, but the notches are detectable by measuring relative changes in the amplitude. In the following amplitude profiles shown in Figs. 3–5, the background amplitude is subtracted from the measured amplitude, and relative change in the amplitude is plotted. Fig. 3 shows the notch-depth dependence of the echo amplitude when the focal point was set to the notches. As the